Phosphoprotein of Human Parainfluenza Virus Type 3 Blocks Autophagosome-Lysosome Fusion to Increase Virus Production

Binbin Ding,[1] Guangyuan Zhang,[1] Xiaodan Yang,[1] Shengwei Zhang,[1] Longyun Chen,[1] Qin Yan,[1] Mengyao Xu,[1] Amiya K. Banerjee,[2] and Mingzhou Chen[1,*]
[1]State Key Laboratory of Virology and Modern Virology Research Center, College of Life Sciences, Wuhan University, LuoJia Hill, Wuhan 430072, People's Republic of China
[2]Department of Molecular Genetics, Lerner Research Institute, Cleveland Clinic, 9500 Euclid Avenue, Cleveland, OH 44195, USA
*Correspondence: chenmz@whu.edu.cn
http://dx.doi.org/10.1016/j.chom.2014.04.004

SUMMARY

Autophagy is a multistep process in which cytoplasmic components, including invading pathogens, are captured by autophagosomes that subsequently fuse with degradative lysosomes. Negative-strand RNA viruses, including paramyxoviruses, have been shown to alter autophagy, but the molecular mechanisms remain largely unknown. We demonstrate that human parainfluenza virus type 3 (HPIV3) induces incomplete autophagy by blocking autophagosome-lysosome fusion, resulting in increased virus production. The viral phosphoprotein (P) is necessary and sufficient to inhibition autophagosome degradation. P binds to SNAP29 and inhibits its interaction with syntaxin17, thereby preventing these two host SNARE proteins from mediating autophagosome-lysome fusion. Incomplete autophagy and resultant autophagosome accumulation increase extracellular viral production but do not affect viral protein synthesis. These findings highlight how viruses can block autophagosome degradation by disrupting the function of SNARE proteins.

INTRODUCTION

Autophagy is a multistep, conserved process by which cytoplasm components, such as damaged organelles and foreign pathogens, become enveloped into double-membrane autophagosome vesicles and shuttled to lysosomes for degradation (Tanida, 2011). Two separate, ubiquitin-like conjugation systems mediate phagophore elongation and the subsequent generation of a double-membraned autophagosome. The first conjugation system contributes to the coupling of Atg12 with Atg5 for forming a covalently linked heterodimer, which then recruits Atg16 to generate phagophores. The second conjugation system couples microtubule-associated protein 1 light chain 3 (LC3) to the phospholipid phosphatidylethanolamine. Finally, the autophagosome fuses with a lysosome to form an autolysosome, where the cytoplasmic material, organelles, or invading pathogens and the inner membrane are degraded. Many proteins required for autophagosome-lysosomal fusion, lysosomal acidification, and lysosomal digestion coordinately contributed to degradation processes.

In recent years, a growing number of studies have suggested that the infection processes of viruses are closely related to the autophagy of host cells, and autophagy can serve as innate immunity and an adaptive immune response against intracellular pathogens (Deretic and Levine, 2009). In addition, intracellular pathogens have developed various molecular strategies to evade or subvert autophagy for their own benefit (Levine, 2005). Many positive RNA viruses exploit the autophagic process for viral RNA replication (Wileman, 2007; Wong et al., 2008). Hepatitis B virus (Sir et al., 2010) and influenza virus (Gannagé et al., 2009) can block the autophagy process to enhance viral replication or dissemination. Furthermore, the induction of autophagy also promotes the replication of these viruses, and the disruption of autophagy results in decreased progeny virus production.

However, within members of nonsegmented negative-strand (NNS) RNA viruses, only few viruses, including vesicular stomatitis virus (VSV) and measles virus (MeV), have been shown to induce autophagy. A recent report indicated that innate recognition of VSV in mouse embryonic fibroblasts (MEFs) via the RIG-I pathway is negatively regulated by the Atg5-Atg12 conjugate. Consequently, $Atg5^{-/-}$ MEFs were more resistant to VSV infection (Jounai et al., 2007). However, another study showed that VSV infection induced autophagy, which in turn activated the antiviral response and inhibited viral replication in the model organism *Drosophila*, and siRNA knockdown of Atg5 increased the yield of progeny viruses (Shelly et al., 2009). Joubert et al. reported that MeV induces autophagy via the engagement of CD46, a cell-surface receptor required for the entry of various pathogens (Joubert et al., 2009). Subsequent research further suggested that both glycoproteins of MeV rapidly induce membrane fusion-mediated autophagy in cells expressing one of the cellular receptors, and MeV requires this induction for efficient cell-to-cell spread (Delpeut et al., 2012). Another study also showed that the C protein of Mev is sufficient to induce autophagosome accumulation through its interaction with immunity-associated GTPase family M (IRGM), and siRNA knockdown of IRGM impairs MeV-induced autophagy and viral particle production (Grégoire et al., 2011). These data indicate that multiple

steps of the autophagy pathway are regulated by paramyxoviruses or other NNS viruses for their own benefit. However, the detailed mechanisms of how paramyxoviruses regulate the autophagic process during infection remain elusive.

Human parainfluenza virus type 3 (HPIV3) is a member of the family *Paramyxoviridae*, order Mononegavirales. During cell infection, an RNA polymerase complex formed by the RNA-dependent RNA polymerase large protein (L) and the phosphoprotein (P) transcribes the N-RNA template to generate six monocistronic mRNAs that are subsequently translated into N, P, matrix (M) protein, fusion protein, hemagglutinin-neuraminidase (HN), and L. The P of paramyxoviruses is a multifunctional protein and has at least three important functions in RNA synthesis: (1) it stabilizes and acts as a cofactor of the L, (2) it mediates specific encapsidation of the viral genome RNA by preventing the N from binding to cellular RNAs, and (3) it acts as a bridge to connect the RNA polymerase complex with the N-RNA template.

HPIV3 is one of the primary pathogens that cause severe respiratory tract diseases including bronchiolitis, pneumonia, and croup in infants and young children. However, no valid antiviral therapy or vaccine is currently available. Thus, a more complete understanding of the factors that influence HPIV3 replication and pathogenesis is therefore necessary to aid in the development of vaccines and antiviral therapies. In this study, we sought to determine how the autophagy process is particularly targeted by HPIV3 and to identify the molecular partners underlying the execution and regulation of the autophagy process between the virus and host. We found that HPIV3 infection blocks autophagosome degradation by inhibiting autophagosome-lysosome fusion, and that the P is necessary and sufficient for this inhibition of autophagosome degradation. Furthermore, we also demonstrated that inhibition autophagosome-lysosome fusion by the P facilitates extracellular viral production but does not influence viral protein synthesis or intracellular viral production.

RESULTS

HPIV3 Infection Triggers the Accumulation of Autophagosomes

To characterize the role of autophagy in the HPIV3 life cycle in detail, we first sought to determine whether HPIV3 infection triggers autophagy. Since the ratio of LC3-I to LC3-II is regarded as an accurate indicator of autophagic activity (Kudchodkar and Levine, 2009), we assessed conversion of endogenous LC3-I to LC3-II via immunoblotting. At 24 hr after HPIV3 infection, LC3-II levels were notably increased in LLC-MK-2 (MK2) cells relative to mock-infected cells and remained constant for 36 hr, whereas the amount of LC3-I decreased at increasing intervals of time following infection (Figure 1A), indicating that there was a cumulative increase in autophagosome formation as infection progressed. Similar results were also observed in HPIV3-infected HeLa cells (Figure 1B), human alveolar adenocarcinoma (A549) cells (see Figure S1A available online), and primary human pulmonary fibroblast (HPF) cells (Figure S1D).

Furthermore, HPIV3 infection led to puncta formation of GFP-LC3-labeled vacuoles in most MK2 and HeLa cells compared with uninfected cells (Figure 1C), confirming that HPIV3 infection indeed induces the formation of autophagosomes. To directly visualize autophagosome formation in HPIV3-infected cells, we also used transmission electron microscopy to observe the ultrastructure of cells. In the mock-infected MK2 cells, autophagic vacuoles were rarely observed (Figure 1D); in contrast, in acidification inhibitors of lysosome degradation, chloroquine (CQ)-treated MK2 cells, a significant increase of single-membrane autophagic vacuoles was observed, and the cytoplasmic contents of most of these vacuoles were sequestered (Figure 1D), Similar results were also observed in CQ-treated U$_2$OS cells (Chen et al., 2012). More remarkably, the accumulation of numerous large, double-membraned autophagic vacuoles containing intact cytoplasmic contents was observed in HPIV3-infected MK2 cells (Figure 1D), suggesting that HPIV3 infection results in autophagosome accumulation. Taken together, these data clearly demonstrate that HPIV3 infection can induce the accumulation of autophagosomes.

HPIV3 Infection Induces Incomplete Autophagy

The accumulation of autophagosomes is an intermediate process within the autophagic flux, which reflects the balance between the rate of their generation and conversion into autolysosomes. Thus, autophagosome accumulation in HPIV3-infected cells may reflect three possibilities: (1) virus induces completed autophagy, (2) the virus simply suppresses basic autophagic flux, or (3) the virus induces incomplete autophagy. To elucidate how HPIV3 infection results in the accumulation of autophagosomes, we first treated mock-and HPIV3-infected cells (moi = 2) with two acidification inhibitors of lysosome degradation, CQ and bafilomycin A1 (BAF), which can suppress autophagic flux and accumulate autoghagosome. If HPIV3 infection only suppresses basic autophagic flux, comparable LC3-II levels will be observed in HPIV3-infected cells and in mock-infected cells upon CQ/BAF treatment. However, we found that higher levels of LC3-II were accumulated in HPIV3-infected cells than in mock-infected cells upon CQ/BAF treatment (Figures 2A and 2B, lanes 2 and 4, and lanes 3 and 5), indicating HPIV3 infection must induce occurrence of the autophagy (either completed autophagy or incomplete autophagy). However, when HPIV3-infected cells (moi = 2) were treated with or without CQ/BAF, no difference in LC3-II levels was observed (Figure 2C, lanes 1 and 2, and lanes 3 and 4), indicating that HPIV3 infection saturates the function of CQ/BAF for blocking the autophagic flux.

Next, we further analyzed the LC3-II and p62 protein levels in the HPIV3-infected cells. Previous studies have shown that the p62 binds to LC3 and that both are degraded in the completed autophagy process after autophagosomes fuse with lysosomes (Bjørkøy et al., 2005). We did not observe any degradation of LC3-II and p62 in HPIV3-infected MK2 cells until 36 hr after infection, although more than 80% of the cells were severely cytopathic (Figure 2D). The similar results were also observed in HPIV3-infected A549 and HPF cells (Figures S1A and S1D). To exclude possible influence of cellular proteins in virus supernatants, MK2 cells were infected with purified HPIV3 for 36 hr, and the results show that purified viruses also prevent autophagosomes from degradation (Figure S1G). To confirm that HPIV3 infection blocks the fusion of autophagosomes with lysosomes, we used a tandem reporter construct, mCherry-GFP-LC3; the GFP of this tandem autophagosome reporter is sensitive and attenuated in an acidic pH environment by lysosomal
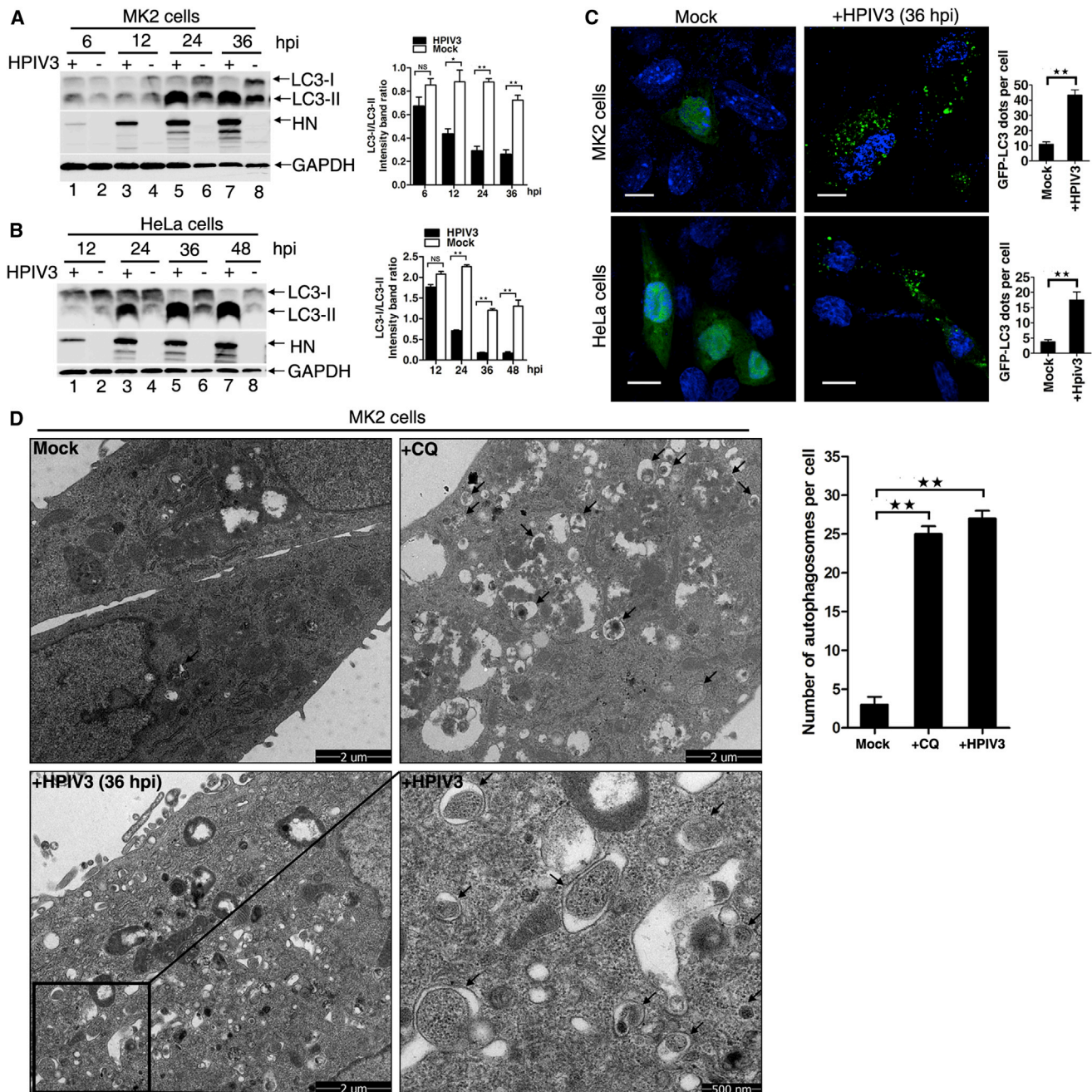
Figure 1. HPIV3 Infection Promotes the Accumulation of Autophagosomes

(A and B) MK2 and HeLa cells were mock infected or infected with HPIV3. Lysates were evaluated via western blotting (WB).

(C) MK2 and HeLa cells were transfected and infected, and analyzed for GFP-LC3. DAPI (blue) was used to stain nuclear DNA. Scale bar, 10 μm. The number of GFP-LC3 dots in each cell was counted, and at least 50 cells were included for each group.

(D) Mock-infected, CQ-treated, or HPIV3-infected MK2 cells were processed and analyzed for the accumulation of autophagosome via electron microscopy. Black arrows indicate autophagic vacuoles.

Error bars, mean ± SD of three experiments. Student's t test; *p < 0.05; **p < 0.01; NS, nonsignificant. See also Figure S1.

degradation, whereas the mCherry is not. Therefore, the fusion of autophagosomes with lysosomes will result in the loss of yellow fluorescence and the appearance of only red fluorescence of mCherry (Klionsky et al., 2012). In HPIV3-infected cells, many LC3-positive autophagic vacuoles were yellow, indicating

that autophagosomes did not fuse with lysosomes (Figures 2E and S1B, left panel), whereas in mock-infected cells there were few yellow autophagic vacuoles, but a high number of mCherry-positive autolysosomes remained detectable. As a positive control, in EBSS-starved cells, which induce a complete
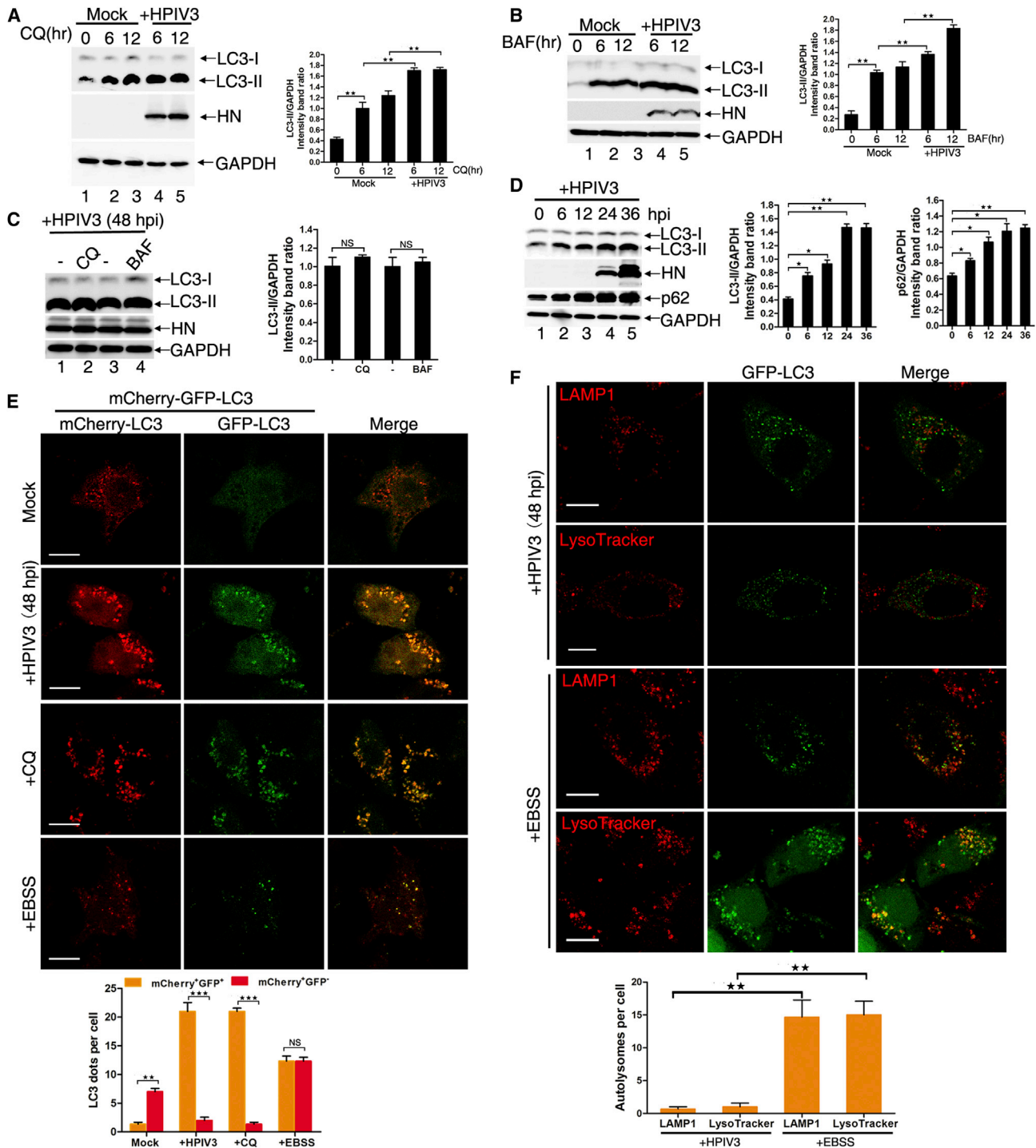
Figure 2. HPIV3 Infection Induces Incomplete Autophagy

(A and B) MK2 cells were mock infected or infected with HPIV3 for 24 hr, and then treated with CQ (A) or BAF (B). Cell lysates were processed as in Figure 1A.

(C) MK2 cells were infected with HPIV3 for 30 hr and treated with/without BAF or CQ, and then processed as in (A).

(D) MK2 cells were infected with HPIV3 and analyzed via WB.

(E) HeLa cells were transfected with mCherry-GFP-LC3 for 24 hr and then were mock infected or infected with HPIV3 or treated with CQ, or starved in EBSS medium for 2 hr, and then analyzed for autophagosome. Scale bar, 10 μm. The graph shows the quantification of autophagosomes by taking the average number of dots in 50 cells.

(F) HeLa cells were transfected and then infected with HPIV3 or starved in EBSS medium for colocalization analysis. Scale bar, 10 μm. The graph shows the quantification of colocalization by taking the average number of dots in 50 cells.

Error bars, mean ± SD of three experiments. Student's t test; **$p < 0.01$; ***$p < 0.001$; NS, nonsignificant. See also Figure S1.

autophagy, only part of the LC3-positive autophagic vacuoles were yellow (Figures 2E and S1B, left panel). Furthermore, we also tracked lysosomes with lysosome-associated membrane protein 1 (LAMP1) and LysoTracker red, which stains acidic organelles such as lysosomes. In HPIV3-infected cells, GFP-LC3 did not colocalize with LAMP1 or LysoTracker red, whereas in starved cells many GFP-LC3 colocalized with LAMP1 or LysoTracker red (Figures 2F; S1B, right panel; and S1E), suggesting that HPIV3 infection indeed blocks the fusion of autophagosomes with lysosomes. Taken together, our results demonstrate that HPIV3 infection induces incomplete autophagy by inhibiting the fusion of autophagosomes with lysosomes.

Accumulation of Autophagosomes Promotes Extracellular Viral Production

Next, we sought to determine whether autophagy machinery could modulate the replication of HPIV3. We first used BAF to inhibit the activity of lysosomes to allow for the accumulation of autophagosomes in the basic autophagy process and rapamycin (RAP), which is a well-known autophagy inducer, to induce the production of autophagosomes. In cells infected with HPIV3 at a lower moi of 0.01, the extracellular viral production (virions released into supernatants) was significantly higher in cells treated with BAF and RAP than in nontreated cells, and viral HN protein expression remained unchanged (Figure 3A); the effect of BAF or RAP treatment on viability of the cells is insignificant (Figures S2A and S2D), but when higher moi (moi = 2) was used, BAF failed to increase the extracellular viral yields because of saturation of blocking autophagosome maturation by higher moi infection (Figure S2G). These results suggest that the accumulation of autophagosomes enhances extracellular viral production but not viral protein synthesis. Next, we treated cells with 3-methyladenine (3-MA), which is a pharmacologic inhibitor of autophagy and inhibits the formation of autophagosomes, and evaluated the effect of 3-MA on viral replication. As shown in Figure 3B, after 48 hr of infection at an moi of 0.01, the level of endogenous LC3-II decreased and the extracellular viral production was three times lower in cells treated with 3-MA than in nontreated cells, whereas HN protein expression remained unchanged; moreover, toxic effects of 3-MA on cells have not been observed at the concentrations used in this study (Figures S2B and S2E). These findings suggest that inhibition of autophagy with 3-MA reduces the extracellular viral production but does not influence viral protein expression. Furthermore, we knocked down expression of the key autophagy-related protein Atg5 via siRNA to inhibit the generation of autophagosomes. The intracellular level of Atg5 protein was reduced to 90% by siRNA (#104) compared with negative control (Figures 3C, S1C, and S1F), and the effect of siRNA treatment on viability of the cells is insignificant (Figures S2C and S2F). As expected, Atg5-knockdown cells lost the ability to accumulate LC3-II even when infected with HPIV3 (Figure 3D, lanes 6 and 8; Figures S1C and S1F); meanwhile, knockdown of Atg5 did not affect HN protein expression or intracellular viral production (virions inside cells) but resulted in a significant reduction in the extracellular viral production (Figures 3D, S1C, and S1F). Similar results were obtained in $Atg7^{-/-}$ (Atg7 knockout) MEF cells infected with HPIV3 (Figure 3E). Taken together, these results suggest that the accumulation of autophagosomes en-

hances extracellular viral production but does not affect the synthesis of viral proteins and intracellular viral production. It has been thought that the M protein of paramyxovirus plays a major role in the process of virion release (Takimoto and Portner, 2004), and our unpublished data also shown that M protein alone of HPIV3 triggers all steps required for the formation and release of virus-like particles (VLPs) that mimic the process of extracellular viral production. To further explore how the accumulation of autophagosomes increases extracellular virus production, we treated cells expressing M protein with BAF or 3-MA and found that BAF enhanced while 3-MA reduced the release of VLPs (Figure 3F), suggesting that accumulation of autophagosomes also increases the release of VLPs, but inhibition of autophagy decreases the release of VLPs; then we performed membrane flotation centrifugation assay and found that M locates both in membrane fractions and nonmembrane fractions (Figure 3G). BAF treatment significantly enhanced the amount of M in membrane fractions compared with mock-treated cells, whereas 3-MA functioned reversely (Figure 3G), suggesting that accumulation of autophagosomes increases the ability of M binding to plasma membrane. Furthermore, we also found that GFP-LC3 colocalized with M in BAF-treated cells (Figure 3H). Taken together, our results indicate that the accumulation of autophagosomes increases the ability of virions binding to membranes, thus increasing extracellular viral yield.

P Is Necessary and Sufficient to Induce Incomplete Autophagy

Next, we sought to determine the mechanism(s) by which HPIV3 infection induces incomplete autophagy. For this purpose, we transiently expressed N, P, M, F, HN, and L of HPIV3, and P expression resulted in a significant increase in LC3-II (Figure 4A). Furthermore, we also observed that the kinetics of P expression parallel the inhibition of autophagosome maturation in HPIV3-infected cells (Figure S3A). Though we are unable to directly detect expression of GFP-L by immune blotting, we do observe the expression of GFP-L by immunefluorescent assay (data not shown). Furthermore, using CQ-treated cells as positive control, the number of autophagosomes was remarkably higher when GFP-LC3 and P were coexpressed than when GFP-LC3 was expressed alone (Figure 4B), indicating that P can trigger the accumulation of autophagosomes. To confirm that expression of P can also induce incomplete autophagy, we first treated cells with CQ or BAF. Levels of LC3-II were higher in the presence of P than in the absence of P (Figure S3B, lanes 2 and 4; Figure S3C). However, LC3-II levels did not increase further in the presence of P upon treatment with CQ (Figure S3B, lanes 3 and 4), indicating that P induces autophagy. Then we sought to determine whether P can also block the fusion of autophagosomes with lysosomes. For this purpose, we cotransfected cells with plasmids encoding mCherry-GFP-LC3 and P, many yellow dots, which represented GFP- and mCherry-positive autophagosomes observed in cells coexpressing mCherry-GFP-LC3 and P, whereas only some mCherry-positive and GFP-negative autophagosomes were found in cells expressing only mCherry-GFP-LC3 (Figure 4C). Furthermore, LAMP1 and LysoTracker red were also used to track the location of lysosomes, and we found that GFP-LC3 did not colocalize with LAMP1 or LysoTracker red in the presence of P (Figure 4D). Similarly, we
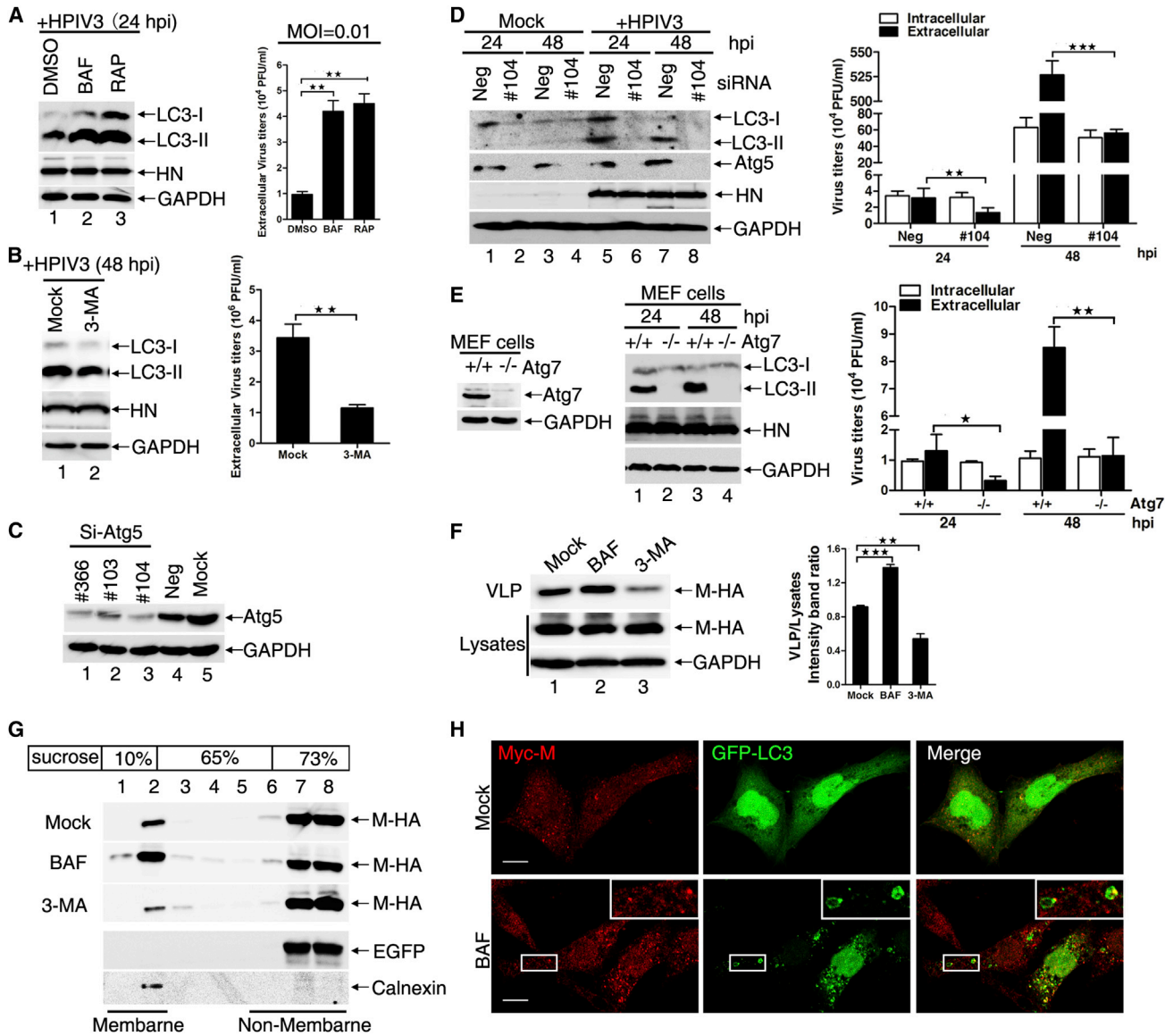
Figure 3. Autophagosome Accumulation Enhances the Extracellulr Viral Yields

(A) MK2 cells were infected with HPIV3 (moi = 0.01) for 24 hr, and treated with BAF or RAP for WB and extracellular viral yields analysis.

(B) MK2 cells were mock infected or treated with 3-MA, and then infected with HPIV3 (moi = 0.01) for 48 hr and analyzed as in (A).

(C) MK2 cells were transfected with siRNAs targeted to Atg5. Lysates were analyzed via WB.

(D) MK2 cells were transfected as in (C) and then were mock infected or infected with HPIV3 (moi = 0.01). Cells were harvested and analysis for WB (right) and intracellular virions production (left).

(E) $Atg7^{-/-}$ (open bars) and $Atg7^{+/+}$ (filled bars) MEF cells were infected with HPIV3. Cells were harvested and analyzed for WB and intracellular virion production.

(F) HEK293T cells were transfected with plasmids encoding M and treated with BAF or 3-MA; culture supernatants were used for VLPs assay.

(G) HEK293T cells were transfected and treated as in (F); lysates were analyzed via membrane flotation centrifugation.

(H) HeLa cells were transfected with GFP-LC3 and Myc-M and then treated with BAF. The colocalization of Myc-M and GFP-LC3-positive autophagosomes was analyzed. Scale bar, 10 μm.

Error bars, mean ± SD of three experiments. Student's t test; *p < 0.05; **p < 0.01; ***p < 0.001. See also Figure S2.

also found that overexpression of P inhibits autophagosome maturation in starved cells (Figure S3D) or RAP-treated cells (Figure S3E). Furthermore, knockdown of P by siRNA also significantly decreased autophagosome accumulation during HPIV3 infection (Figures S3F and S3G). Taken together, these data demonstrate that P is sufficient to induce incomplete autophagy by blocking the fusion of autophagosomes with lysosomes.

P Interacts with SNAP29

Next, we sought to determine the mechanism(s) by which P blocks the fusion of autophagosomes with lysosomes. We first screened a HeLa cell cDNA library using P as a bait protein in a yeast two-hybrid system, and a synaptosome-associated protein of 29 kDa (SNAP29), which belongs to family of soluble N-ethylmaleimide-sensitive factor-attachment protein receptors
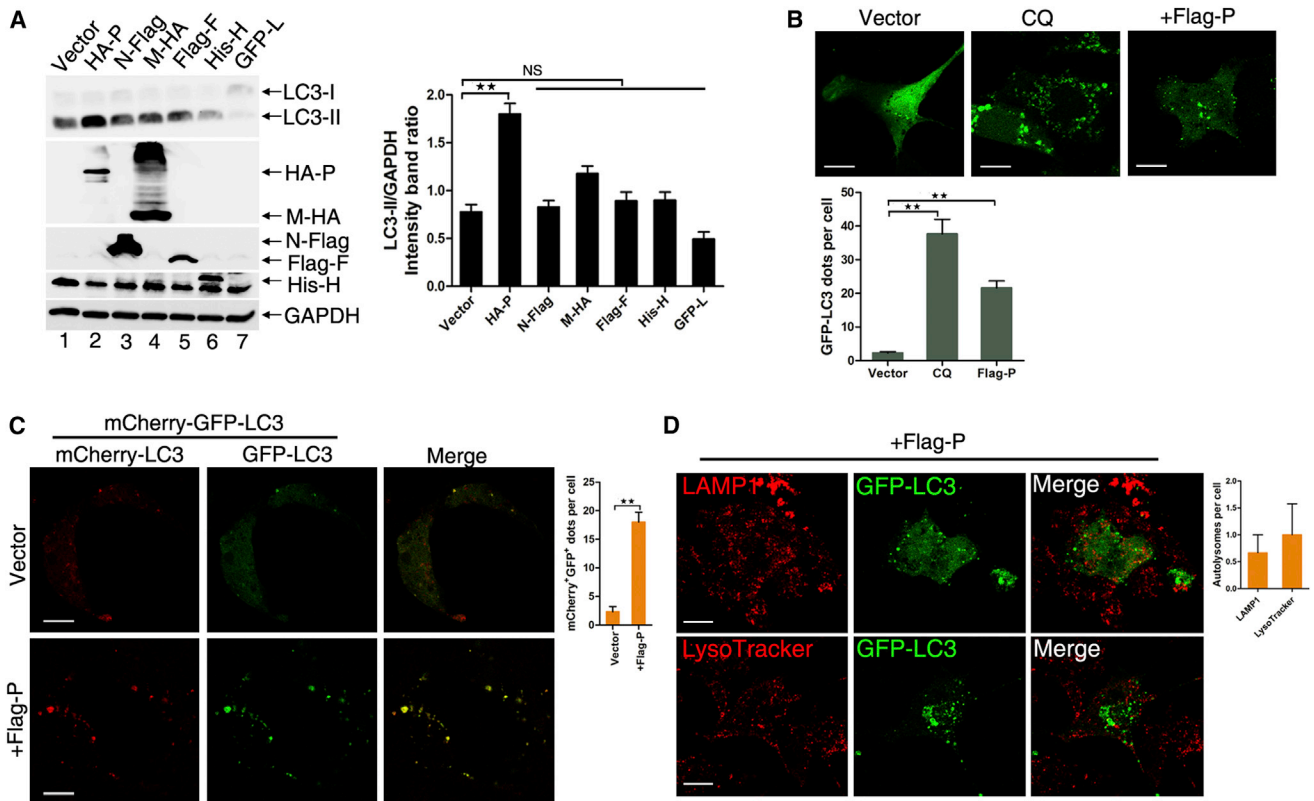
Figure 4. P Inhibits the Fusion of Autophagsosome with Lysosomes

(A) HeLa cells were transfected with plasmids encoding P, N, M, F, H, and L for 36 hr; lysates were analyzed via WB.

(B) HeLa cells were cotransfected with plasmids as indicated in the presence of CQ. Cells were analyzed for autophagosome. Scale bar, 10 μm.

(C) HeLa cells were cotransfected with plasmids as indicated and analyzed for autophagosome. Scale bar, 10 μm. The graph shows the quantification of mCherry$^+$GFP$^+$-LC3-positive autophagosomes by taking the average number of dots in 30 cells. Student's t test; **p < 0.01.

(D) HeLa cells were cotransfected with plasmids as indicated for colocalization assay. Scale bar, 10 μm. The graph shows the quantification of colocalization by taking the average number of dots in 30 cells.

Error bars, mean ± SD of three experiments. Student's t test; *p < 0.05; **p < 0.01; ***p < 0.001. See also Figure S3.

(SNAREs), was found to specifically interact with P (Figure 5A). Then we performed in vivo coimmunoprecipitation (coIP). As shown in Figure 5B, HA-SNAP29 coimmunoprecipitated with Myc-P (right panel, lane 2). We also observed that endogenous SNAP29 coimmunoprecipitated with Flag-P in HEK293T cells (Figure 5C, lane 2) and colocalized well with Flag-P in HeLa cells via immunofluorescence assay (Figure 5D). To further confirm that SNAP29 interacts with P, we performed an in vitro GST pull-down assay with GST-fused SNAP29 expressed in bacteria. GST-SNAP29, but not GST alone, was able to pull down P (Figure 5E). Taken together, these results confirm that P and SNAP29 physically and specifically interact in vivo and in vitro.

Next, to map the critical region of P necessary for its interaction with SNAP29, a series of progressively truncated P mutants were constructed (Figure 5F, upper panel) and used for coIP assay. We found that mutant Myc-PΔN100 failed to coimmunoprecipitate HA-SNAP29 (Figure 5F, bottom right panel, lanes 2–5) but still maintained the ability of oligomerization and interaction of PΔN100 with N (Figure S4, right panel, lanes 3 and 5), suggesting N-terminal 100 aa is indeed required for regulating the interaction of P with SNAP29.

SNAP29 contains two SNARE motifs (aa 60–112 and aa 206–258) (Hong, 2005). To map the critical region of SNAP29 responsible for its interaction with P, we also constructed a series of SNAP29 truncation mutants (Figure 5G, upper panel) and performed coIP assay. The results showed that deletion or truncation of one of the SNARE motifs of SNAP29 definitely abolished the interaction of SNAP29 with P (Figure 5G, right bottom panel). Altogether, these data indicate that both SNARE motifs in SNAP29 are required for its interaction with P.

P Blocks Autophagosome-Lysosome Fusion by Inhibiting SNAP29 Interaction with Syntaxin17

Recently, an elegant study showed that SNAP29 is a key adaptor protein in regulating the fusion of autophagosomes with lysosomes by interacting with syntaxin17 (Stx17), which targets autophagosomes, and VAMP8, which locates in the membranes of lysosomes (Itakura et al., 2012). Indeed, as previously reported (Itakura et al., 2012), knockdown of SNAP29 by siRNA caused dramatic accumulation of GFP-LC3 dots (Figure 6A) and LC3-II in MK2 cells even under normal conditions (Figure 6B, lanes 2 and 4), suggesting knockdown of SNAP29 inhibits the fusion of autophagosomes with lysosomes. However, in
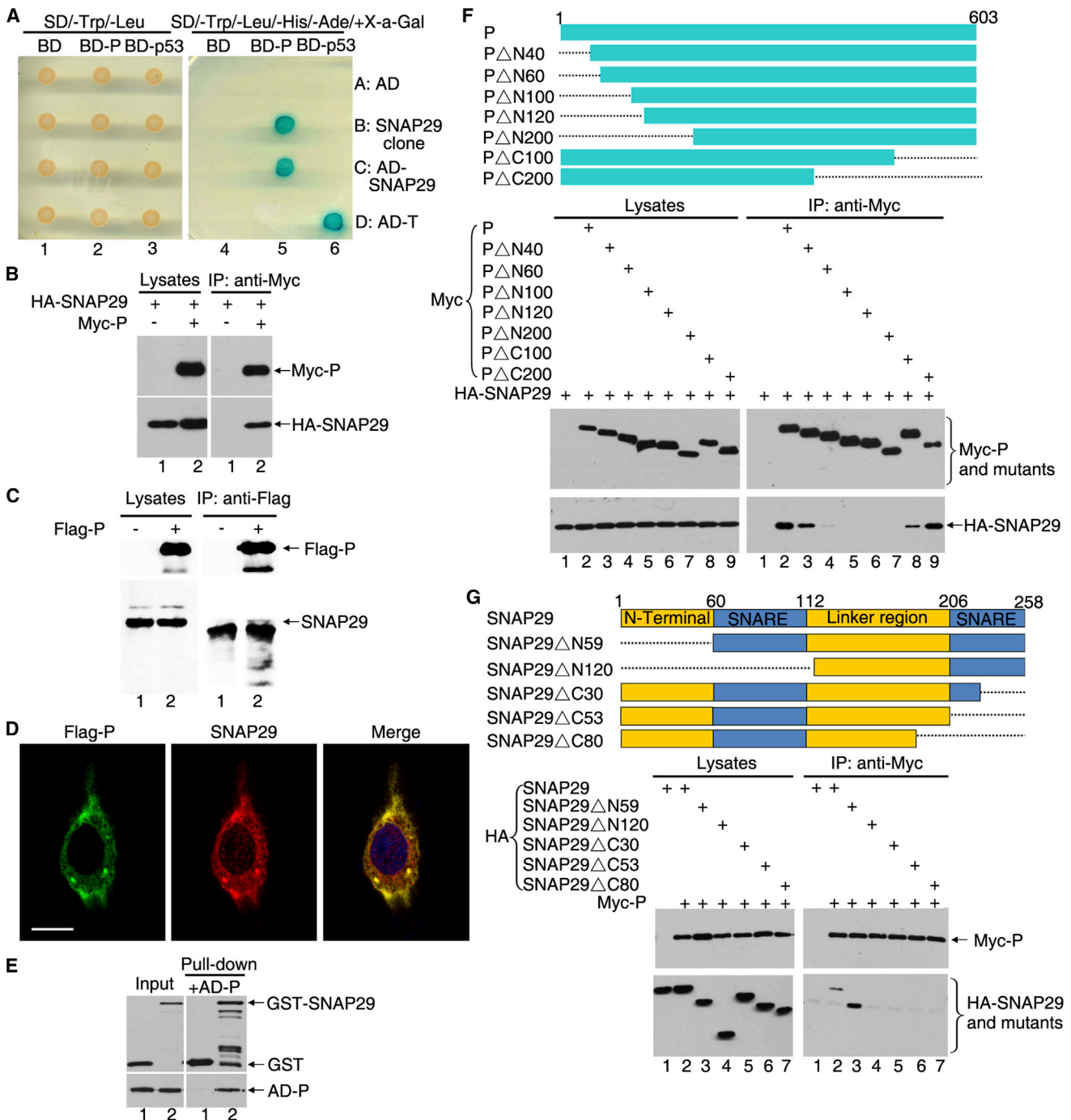
Figure 5. P Interacts with SNAP29

(A) P interacts with SNAP29 in yeast.

(B) HA-SNAP29 was expressed alone or coexpressed with Myc-P. Cell lysates were subjected to IP and analyzed via WB.

(C) HEK293T cells were transfected with plasmid encoding Flag-P. Lysates were subjected to IP and analyzed via WB.

(D) MK2 cells were transfected with plasmid encoding Flag-P and analyzed for colocalization of Flag-P with endogenous SNAP29. Scale bar, 10 μm.

(E) GST or GST-SNAP29 was expressed in bacteria, and lysates containing GST or GST-SNAP29 were used for the binding of HA-P and analyzed via WB.

(F) HA-SNAP29 was expressed as indicated, and the cell lysates were processed as in (B).

(G) Myc-P was coexpressed as indicated, and the cell lysates were processed as in (B). See also Figure S4.

higher-moi (moi = 2) HPIV3-infected cells, LC3-II levels did not further increase regardless of whether SNAP29 was knocked down (Figure 6B, lanes 1 and 3), further suggesting HPIV3 infec-

tion is sufficient to block the fusion of autophagosomes with lysosomes. Furthermore, the accumulation of autophagosomes via SNAP29 knockdown also resulted in a 4-fold increase of
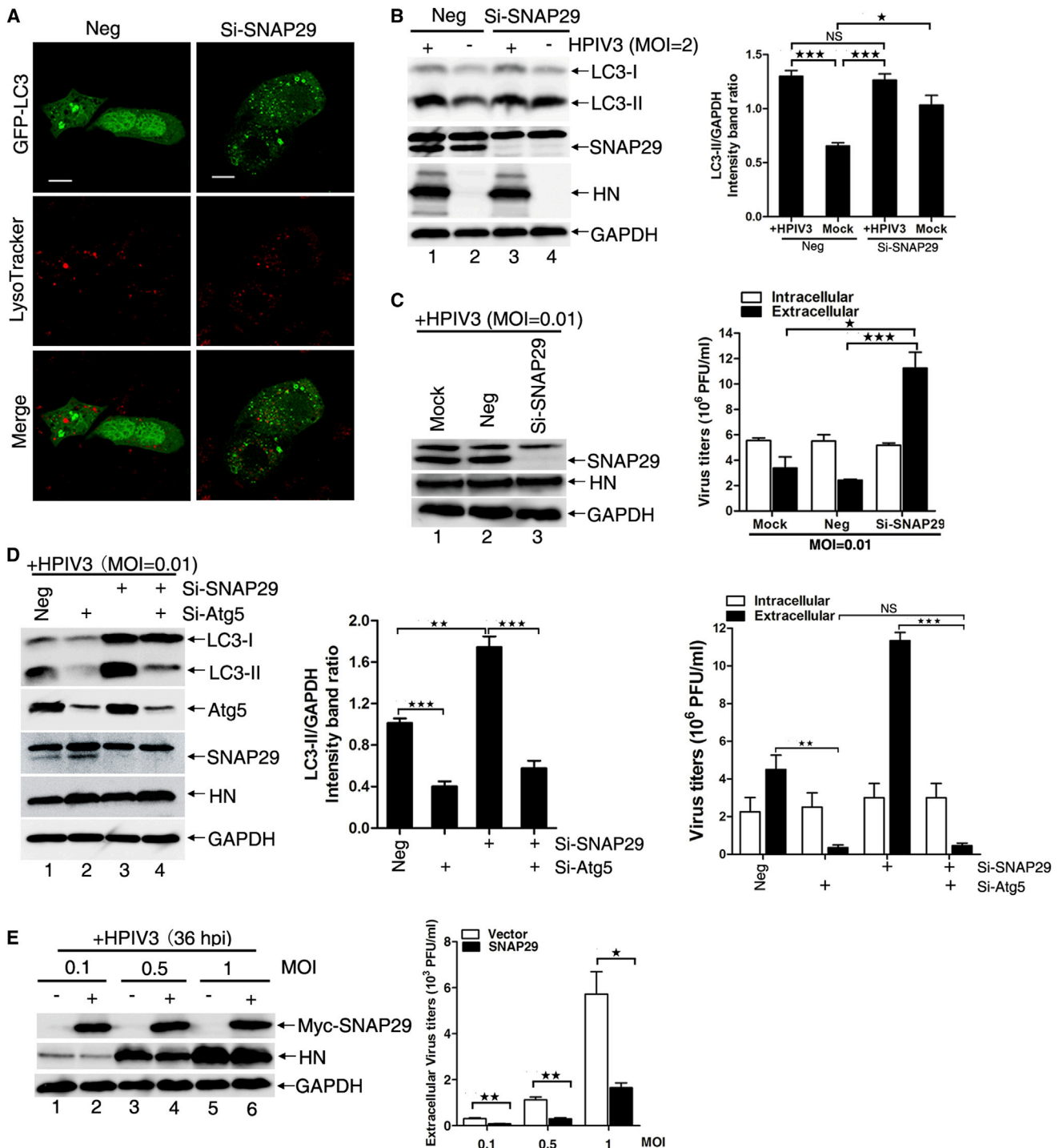
Figure 6. Knockdown or Overexpression of SNAP29 Affects Extracellular HPIV3 Yields

(A) MK2 cells were transfected with siRNA for SNAP29 for 48 hr and were transfected with plasmid encoding GFP-LC3 for an additional 24 hr for colocalization assay. Scale bar, 10 μm. One of three experiments is shown.

(B) MK2 cells were transfected as in (A), and cells were mock infected or infected with HPIV3 for 36 hr and analyzed via WB.

(C) MK2 cells were transfected and infected as in (B), but at an moi of 0.01. Cells were harvested and analyzed for WB and intracellular virion production.

(D) MK2 cells were transfected with siRNAs as indicated for 48 hr, and then cells were mock infected or infected with HPIV3 (moi = 0.01) for 36 hr. Cells were harvested and analysis for WB and intracellular and extracellular virions production.

(E) HeLa cells were transfected with plasmid encoding Myc-SNAP29 for 24 hr and infected with HPIV3 at an moi of 0.1, 0.5, or 1 for 48 hr, and then processed as in (C).

Error bars, mean ± SD of three experiments. Student's t test; *p < 0.05; **p < 0.01; ***p < 0.001; NS, nonsignificant. See also Figure S5.

extracellular viral yields in lower moi (moi = 0.01) (Figure 6C), but not in higher moi (moi = 2) (Figure S5) HPIV3-infected cells, whereas HN expression and intracellular viral yield were not affected. However, double knockdown of Atg5 and SNAP29, which has no significant effect on viability of cells (Figures S2C and S2F), completely cut off the effect of single silence of SNAP29 on extracellular viral production, and resulted in comparable extracellular viral production with single silence of ATG5 (Figure 6D), suggesting that SNAP29 regulates extracellular viral production only through blocking fusion of autophagosomes with lysosomes, and silence of ATG5 blocks the early stage of autophagy, with the result that autophagosomes cannot form. Furthermore, overexpression of SNAP29 reduced the extracellular viral yield compared with mock-transfected cells (Figure 6E). Altogether, these results shown that SNAP29 has an important function in regulating the fusion of autophagosomes with lysosomes and that the accumulation of autophagosomes increases extracellular viral yield.

Both HPIV3 infection and P expression can block the fusion of autophagosomes with lysosomes; meanwhile, P interacts with SNAP29, which is the key adaptor protein in regulating the fusion of autophagosomes with lysosomes. Thus, we sought to determine whether P blocks the fusion of autophagosomes with lysosomes by disrupting the function of SNAP29 in HPIV3-infected cells. For this purpose, we first infected HEK293T cells, which coexpressed Myc-SNAP29 and HA-Stx17, and as shown in Figure 7A, infection with HPIV3 greatly weakened the association of SNAP29 with Stx17 (right bottom panel, lanes 2 and 3) but did not influence the interaction of SNAP29 with VAMP8 (Figure 7B, right bottom panel, lanes 2 and 3), indicating that HPIV3 infection suppresses the interaction of SNAP29 and Stx17, which is critical for the fusion of autophagosomes with lysosomes.

Furthermore, expression of HA-P also remarkably inhibited the interaction of SNAP29 with Stx17 (Figure 7C, right bottom panel, lane 3), but expression of HA-PΔN100, which lost the ability to interact with SNAP29, failed to inhibit the interaction of SNAP29 with Stx17 (Figure 7C, right bottom panel, lane 4). Consistent with these data, HA-PΔN100 was also unable to promote the accumulation of LC3-II (Figure 7D, lanes 2 and 3). Furthermore, transmission electron microscopy was used to observe the ultrastructure of HeLa cells expressing HA-P or HA-PΔN100. Higher-magnification images clearly showed double-membraned vesicles with cytoplasmic contents, which are indicative of autophagosomes, in HeLa cells expressing HA-P, but not in cells expressing HA-PΔN100 (Figure 7E). By quantifying autophagic vesicles, we found that the number of autophagosomes was six times greater in HeLa cells expressing HA-P than in those expressing HA-PΔN100 (Figure 7E).

Because the two SNARE motifs of SNAP29 are both required for its interaction with P (Figure 5G), we next sought to determine whether P blocks the interaction of SNAP29 with Stx17 by competitively binding SNARE motifs. Two mutants, SNAP29ΔN120 and SNAP29ΔC80, in which one of the two SNARE motifs was deleted, were chosen as the representatives for coIP assay, which showed that neither SNAP29ΔN120 nor SNAP29ΔC80 interacted with Stx17 (Figure 7F and Figure S6A, right bottom panel, lanes 2–4), suggesting that the two SNARE motifs are both required for the interaction of SNAP29 with Stx17. To confirm that P blocks the fusion of autophagosomes with lysosomes by competitively inhibiting the interaction of SNAP29 with Stx17, we gradually increased the expression of SNAP29 and found that the P-induced LC3-II accumulation was reversed (Figure S6B, lanes 3–6). Taken together, our data show that the two SNARE motifs of SNAP29 are both required for SNAP29-P interaction and SNAP29-Stx17 interaction, and that P of HPIV3 blocks the fusion of autophagosomes with lysosomes by inhibiting the interaction of SNAP29 with Stx17.

DISCUSSION

Adaptor protein SNAP29 is indispensible for regulating the fusion of autophagosomes with autolysosomes through SNAP29-Stx17 interaction and SNAP29-VAMP8 interaction (Itakura et al., 2012). From our findings, we can conclude that the HPIV3 infection or P induced incomplete autophagy by blocking SNAP29-mediated fusion of autophagosomes with lysosomes (Figure 7G). We also showed that N-terminal 100 aa of P is indispensible for the competitive binding two SNARE motifs of SNAP29 with Stx17 for efficient blockage of autophagosomes fusion with lysosomes (Figure 7G), which finally facilitates extracellular viral production, but not protein synthesis and intracellular viral production.

As a SNARE protein, SNAP29 was initially identified by yeast two-hybrid screening and was localized predominantly in intracellular membrane structures (Steegmaier et al., 1998). Due to its ubiquitous cytoplasmic expression and interactions with a broad range of syntaxin proteins, SNAP29 has been considered to be capable of participating in various intracellular transport steps (Hohenstein and Roche, 2001). A recent study shows that SNAP29 interacts with the BLOC1 complex that is responsible for specialized cargo sorting in the endosome-to-Golgi retrograde trafficking pathway (Gokhale et al., 2012). In addition, it has also been reported that SNAP29 may inhibit SNARE complex disassembly (Su et al., 2001). Furthermore, a recent study greatly expands the function of SNAP29, which suggested that SNAP29 regulates fusion of autophagosomes with lysosomes through SNAP29-Stx17 interaction and SNAP29-VAMP8 interaction (Itakura et al., 2012).

Our results show that HPIV3 infection or the expression of P can induce incomplete autophagy. Although we observed that P plays a key role in the induction of incomplete autophagy, other viral proteins or ingredients may synergistically contribute to this process in viral infection. Others have speculated that autophagy promotes viral replication through multiple mechanisms including inhibiting the innate immune response (Estrabaud et al., 2011; Ke and Chen, 2011), stimulating protein translation (Dreux et al., 2009), and generating energy or membrane structures required for viral replication (Heaton and Randall, 2010). In our study, we discovered that autophagosome accumulation enhanced the extracellular viral yields of HPIV3 (Figure 3A). Furthermore, inhibition of autophagy reduced the extracellular viral yields (Figures 3B and S2H), but protein composition and infectivity of released virions were not affected (Figures S2I–S2K). Similarly, other studies have suggested that HCV RNA in cells induces an incomplete autophagic response that promotes viral RNA replication (Sir et al., 2008) and that siRNA knockdown of Atg7 decreases the production of infectious HCV particles,
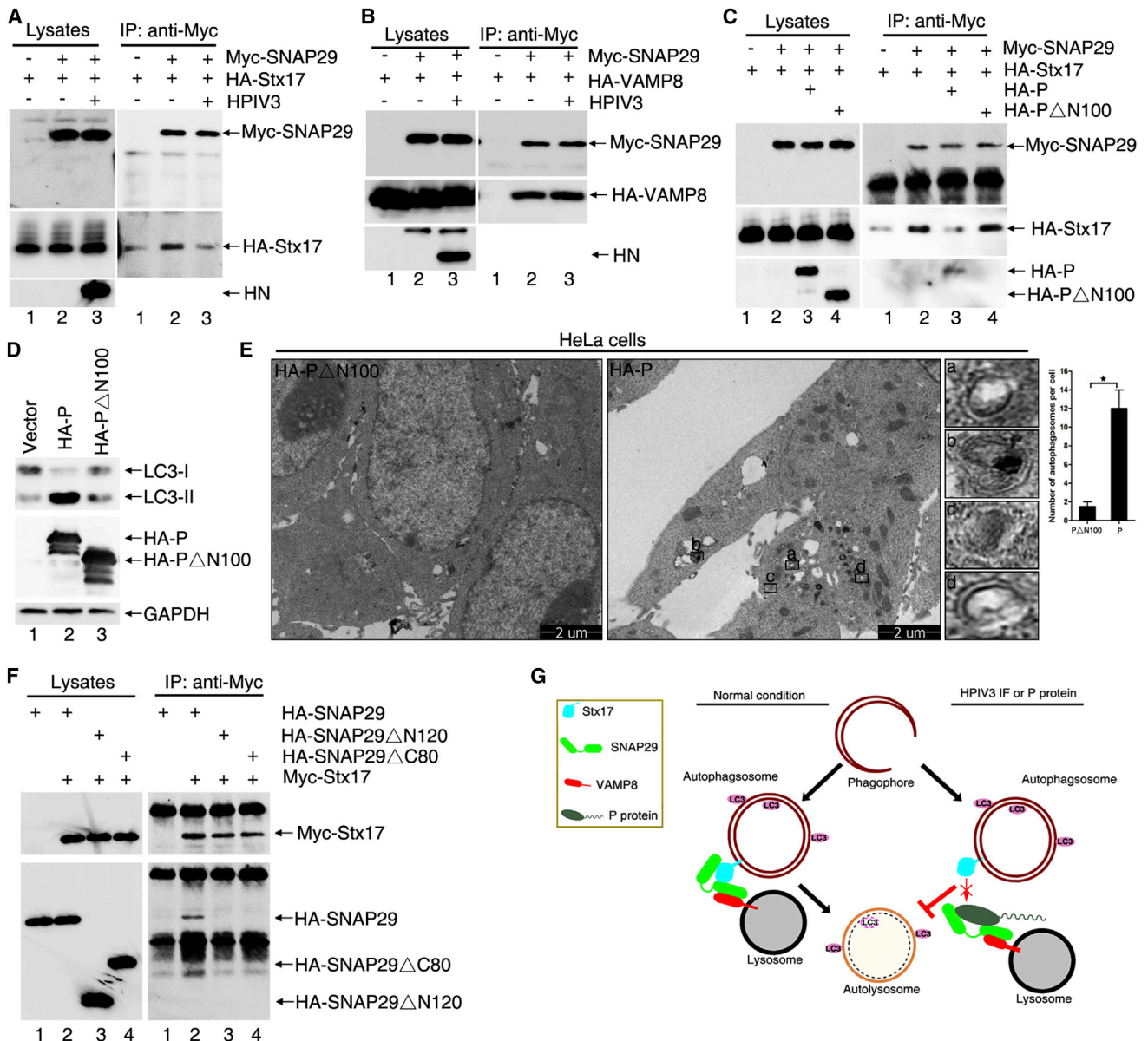
Figure 7. P Blocks the Interaction of SNAP29 with Stx17

(A) HEK293T cells were transfected as indicated and were mock infected or infected by HPIV3. Lysates were processed as in Figure 5B.

(B) HEK293T cells were transfected as indicated and infected as in (A). Cell lysates were processed as in (A).

(C) HEK293T cells were transfected as indicated, and cell lysates were processed as in (A).

(D) HEK293T cells were transfected as indicated, and cell lysates were analyzed via WB.

(E) HeLa cells were transfected as indicated and then processed and analyzed for the autophagosome. Rectangle indicates autophagosomes.

(F) HeLa cells were transfected as indicated, and cell lysates were processed as in (A).

(G) Model of HPIV3 infection or P induced-incomplete autophagy.

Student's t test; *p < 0.05. See also Figure S6.

with no apparent effects on the expression of viral RNA and proteins (Tanida et al., 2009); coxsackievirus B3-induced autophagy can enhance viral replication, and the inhibition of autophagosome formation via pharmacological compounds or siRNA knockdown of autophagy-related genes can reduce viral production. However, blocking the fusion of autophagosomes with lysosomes by silencing LAMP2 significantly increased virus titer (Wong et al., 2008).

To confirm that HPIV3-induced incomplete autophagy only contributes to extracellular viral yields rather than intracellular virion production, we also assessed intracellular viral yields and consistently observed a more substantial effect on extracellular viral yield than intracellular viral yields when accumulation of autophagosome was induced or inhibited (Figures 3D, 3E, 6C, and 6D), suggesting that HPIV3 does not require a functional autophagy pathway for transcription and replication. The

positive correlations between the decreased accumulation of autophagosomes and decreased extracellular viral yield led us to conclude that the autophagosome accumulation induced during HPIV3 infection increases extracellular viral yields, and we hypothesize that HPIV3 subverts the constituents of the cellular autophagy pathway to form membranous scaffolds for the intracellular transportation or budding of virions. A previous study revealed a similar phenomenon for nonenveloped viruses such as poliovirus: a larger effect on extracellular viral yield than intracellular viral yield was observed after siRNA knockdown of Atg12 and LC3, indicating that poliovirus has a selective effect on viral release and that poliovirus may use a double-membraned autophagosome-mediated pathway as a nonlytic mechanism for viral release (Jackson et al., 2005; Taylor et al., 2009). Thus, the intracellular accumulation of autophagosomes in HPIV3-infected cells (like poliovirus-infected cells) may provide a nonlytic release pathway for the extracellular delivery of cytosolic contents in the absence of cell lysis. Similarly, some enveloped viruses, such as HIV, have also been suggested to egress from human macrophages via the fusion of multivesicular bodies with plasma membrane, rather than by directly budding from the cell surface as in HIV-infected T cells (Pelchen-Matthews et al., 2003; Nydegger et al., 2003; Ono and Freed, 2004). Whatever HPIV3 employs lytic or nonlytic release pathway for release of virions, this raises one question: how do virions of HPIV3 connect with autophagosomes? We further found that accumulation of autophagosomes increases the VLPs release of M protein and ability of M binding to membranes, and M protein colocalizes with autophagosome, suggesting that autophagosomes may sequester and facilitate the virions binding to membrane for extracellular viral production. It has been suggested that the accumulation of autophagosomes may contribute to autophagy-mediated secretory functions in response to viral infection and autophagy machinery might also be involved in the regulation of intracellular trafficking, secretion, or exocytosis (Deretic et al., 2012).

Because the fusion of autophagosomes with lysosomes is a main step in the autophagic flux, many regulators of autophagosome maturation and degradation, such as UVRAG, Rubicon, Beclin-1, presenilin-1, and valosin-containing protein, have been identified (Liang et al., 2008; Matsunaga et al., 2009; Lee et al., 2010; Tresse et al., 2010). Viruses might disrupt this process for their benefit by interfering with the function of these regulators. For example, M2 protein of influenza virus A blocks the fusion between autophagosomes and lysosomes via its interaction with Beclin-1 in MEF cells (Gannagé et al., 2009); Nef protein of HIV-1 also suppresses autophagic maturation and causes the accumulation of autophagosomes by interacting with Beclin-1 in U937 cell lines (Kyei et al., 2009). Similarly, NSP4 protein of rotavirus binds to autophagosomes and inhibits their fusion with lysosomes to enhance viral RNA replication, but critical regulators to which NSP4 binds have not yet been identified (Berkova et al., 2006). Here, we found that the interaction of P with SNAP29 through two SNARE motifs of SNAP29 disrupts the fusion of autophagosomes with lysosomes for efficient extracellular viral production. Intriguingly, we found that P competitively binds to two SNARE motifs of SNAP29 with Stx17. Because other studies have suggested that other SNARE proteins are also critical for regulating the fusion of autophagosomes with

lysosomes (Fader et al., 2009; Moreau et al., 2011) and for recruiting the LC3 to the site of autophagosome formation (Nair et al., 2011), these SNARE proteins might also be targets for various viruses to block the autophagy maturation for their own benefit.

In summary, we demonstrate that P of HPIV3 interacts with a key adaptor protein, SNAP29, to block autophagosome degradation for efficient budding. Our study introduces a mechanism by which viruses interfere with function of the SNARE protein to disrupt autophagy maturation.

EXPERIMENTAL PROCEDURES

SDS-PAGE and WB

Cells were harvested and lysed with 100 μl of lysis buffer for 30 min at 4°C. The supernatants were collected by centrifugation for 30 min at 4°C. Protein concentration was determined based on the Bradford method using the Bio-Rad protein assay kit. Equal amounts of protein were separated by 12% SDS-PAGE and electrophoretically transferred onto a nitrocellulose membrane (GE Healthcare). After blocking with 5% nonfat milk in PBST, membrane was incubated with the primary antibodies, followed by HRP-conjugated goat anti-rabbit or anti-mouse IgG.

Immunofluorescence Analysis

Cells were fixed with ice-cold 4% (wt/vol) paraformaldehyde for 20 min in room temperature, and then cells were incubated with 0.1% Triton X-100 for 20 min and blocked with 3% BSA for 30 min. Specific primary Abs were added and incubated for 1 hr, and cells were then washed with 1% BSA for three times, followed by incubation with the goat anti-rabbit IgG Rhodamine or goat anti-mouse IgG fluorescein secondary antibody for 1 hr. DAPI was used to stain the nucleus for 5 min.

Yeast Two-Hybrid Screening

Plasmids encoding DNA binding domain (BD) fused with P of HPIV3 were transformed into *Saccharomyces cerevisiae* AH109 (type a) and were used as a bait protein to screen a human HeLa MATCHMAKER cDNA library cloned into a pGADT7-Rec vector (Clontech) according to the manufacturer's protocol. The specificity of the interaction was confirmed by retransforming AD-SNAP29 into Y187 (type α) yeast cells and remating with BD-P expressed in AH109 yeast cells. The mating cultures were coated onto SD/−Trp/−Leu plate for diploid cell growth and onto SD/−Trp/−Leu/−His/−Ade plate containing X-α-Gal for detecting blue colony growth to select protein interaction.

In Vivo Coimmunoprecipitation

HeLa cells were infected with vTF7-3 at an moi of 3 for 1 hr, and transfected with the appropriate plasmids with Lipofectamine 2000 (Invitrogen) according to the manufacturer's protocol; HEK293T cells were transfected with the appropriate plasmids by standard calcium phosphate precipitation method. Cells were harvested and lysed with lysis buffer (50 mM Tris-HCl [pH 7.4], 150 mM NaCl, 1% [wt/vol] Triton X-100, 1 mM EDTA [pH 8.0], 0.1% [vol/vol] SDS, and protease inhibitor cocktail) for 30 min. The supernatants were collected by centrifugation at 13,000 rpm for 30 min at 4°C and precleared by incubated with protein G Sepharose 4 Fast Flow beads for 1 hr at 4°C with rotation. After centrifugation, specific primary antibodies were added in supernatants and incubated for 4 hr at 4°C with rotation, and then the protein G Sepharose 4 Fast Flow beads were added and incubated overnight at 4°C with rotation. Beads were collected and washed three times with washing buffer (5% [wt/vol] sucrose, 5 mM Tris-HCl [pH 7.4], 5 mM EDTA [pH 8.0], 500 mM NaCl, 1% [vol/vol] Triton X-100). Then the beads were boiled at 100°C for 5 min in 2 × SDS protein loading buffer and analyzed by WB.

GST Pull-Down Assays

GST or GST-SNAP29 was expressed in BL21 cells, treated with the lysis buffer provided by a ProFound GST pull-down protein-protein interaction kit (Pierce), and incubated for 30 min at room temperature. After centrifugation at 13,000 rpm for 30 min, equal amounts of supernatants were mixed with P

from HeLa lysates. GST pull-down assays were performed with a ProFound GST pull-down protein-protein interaction kit according to the manufacturer's protocol.

Transmission Electron Microscopy

MK2 cells was infected by HPIV3 for 36 hr at an moi of 2 or treated with CQ (50 μM) for 6 hr; HeLa cells were transfected by pCAGGS-HA-P or PΔN100 for 36 hr, and then cells were fixed with 2.5% glutaraldehyde and 4% paraformaldehyde in 0.1 M sodium phosphate buffer (pH 7.4) for 2 hr at room temperature. The cells were harvested and fixed with 2.5% glutaraldehyde on ice for 2 hr followed by postfixation in 2% osmium tetroxide, and then cells were dehydrated with sequential washes in 50%, 70%, 90%, 95%, and 100% ethanol. Areas containing cells were block mounted and thinly sliced.

Autophagy Analysis

For RAP (100 nM), CQ (50 μM), or BAF (100 nM), cells were treated for 6 hr before harvest. For 3-MA (5 mM), cells were pretreated for 2 hr and treated again after absorption of HPIV3 until the samples were harvested. For starvation assay, cells were washed three times with PBS and then cultured in EBSS for 2 hr.

Virus-like Particle Assays

HEK293T cells were transfected with indicated plasmids, 2 ml culture supernatants were recovered and loaded onto 2 ml 20% (w/v) sucrose solutions and centrifuged at 35,000 rpm for 2 hr at 4°C, and pellets were resuspended in PBS at 4°C overnight for WB.

Membrane Flotation Centrifugation

HEK293T cells were transfected with indicated plasmids for 48 hr and were Dounce homogenized in cold TNE buffer (50 mM Tris-HCl, 150 mM NaCl, 2 mM EDTA, 0.1% 2-mercaptoethanol and protease inhibitors cocktail) for 20 min. The supernatants were collected after centrifugation at 3,000 rpm for 30 min at 4°C and mixed with sucrose solution to obtain 73% final concentration. A total of 1 ml of mixture at the bottom was layered with 3 ml 65% (w/v) and 0.8 ml 10% (w/v) sucrose solutions and centrifuged at 28,800 rpm for 16 hr at 4°C. Eight fractions (0.6 ml/fraction) were collected from the top to bottom, and proteins were extracted with methanol/chloroform for WB.

Statistical Analysis

Data are expressed as means ± SD. The significance of the variability between different groups was determined by two-way ANOVA tests of variance using the GraphPad Prism software (version 5.0). $p < 0.05$ was considered statistically significant, and $p > 0.05$ was considered statistically nonsignificant.

SUPPLEMENTAL INFORMATION

Supplemental Information includes six figures and Supplemental Experimental Procedures and can be found with this article at http://dx.doi.org/10.1016/j.chom.2014.04.004.

REFERENCES

Berkova, Z., Crawford, S.E., Trugnan, G., Yoshimori, T., Morris, A.P., and Estes, M.K. (2006). Rotavirus NSP4 induces a novel vesicular compartment regulated by calcium and associated with viroplasms. J. Virol. *80*, 6061–6071.

Bjørkøy, G., Lamark, T., Brech, A., Outzen, H., Perander, M., Overvatn, A., Stenmark, H., and Johansen, T. (2005). p62/SQSTM1 forms protein aggregates degraded by autophagy and has a protective effect on huntingtin-induced cell death. J. Cell Biol. *171*, 603–614.

Chen, D., Fan, W., Lu, Y., Ding, X., Chen, S., and Zhong, Q. (2012). A mammalian autophagosome maturation mechanism mediated by TECPR1 and the Atg12-Atg5 conjugate. Mol. Cell *45*, 629–641.

Delpeut, S., Rudd, P.A., Labonté, P., and von Messling, V. (2012). Membrane fusion-mediated autophagy induction enhances morbillivirus cell-to-cell spread. J. Virol. *86*, 8527–8535.

Deretic, V., and Levine, B. (2009). Autophagy, immunity, and microbial adaptations. Cell Host Microbe *5*, 527–549.

Deretic, V., Jiang, S., and Dupont, N. (2012). Autophagy intersections with conventional and unconventional secretion in tissue development, remodeling and inflammation. Trends Cell Biol. *22*, 397–406.

Dreux, M., Gastaminza, P., Wieland, S.F., and Chisari, F.V. (2009). The autophagy machinery is required to initiate hepatitis C virus replication. Proc. Natl. Acad. Sci. USA *106*, 14046–14051.

Estrabaud, E., De Muynck, S., and Asselah, T. (2011). Activation of unfolded protein response and autophagy during HCV infection modulates innate immune response. J. Hepatol. *55*, 1150–1153.

Fader, C.M., Sánchez, D.G., Mestre, M.B., and Colombo, M.I. (2009). TI-VAMP/VAMP7 and VAMP3/cellubrevin: two v-SNARE proteins involved in specific steps of the autophagy/multivesicular body pathways. Biochim. Biophys. Acta *1793*, 1901–1916.

Gannagé, M., Dormann, D., Albrecht, R., Dengjel, J., Torossi, T., Rämer, P.C., Lee, M., Strowig, T., Arrey, F., Conenello, G., et al. (2009). Matrix protein 2 of influenza A virus blocks autophagosome fusion with lysosomes. Cell Host Microbe *6*, 367–380.

Gokhale, A., Larimore, J., Werner, E., So, L., Moreno-De-Luca, A., Lese-Martin, C., Lupashin, V.V., Smith, Y., and Faundez, V. (2012). Quantitative proteomic and genetic analyses of the schizophrenia susceptibility factor dysbindin identify novel roles of the biogenesis of lysosome-related organelles complex 1. J. Neurosci. *32*, 3697–3711.

Grégoire, I.P., Richetta, C., Meyniel-Schicklin, L., Borel, S., Pradezynski, F., Diaz, O., Deloire, A., Azocar, O., Baguet, J., Le Breton, M., et al. (2011). IRGM is a common target of RNA viruses that subvert the autophagy network. PLoS Pathog. *7*, e1002422.

Heaton, N.S., and Randall, G. (2010). Dengue virus-induced autophagy regulates lipid metabolism. Cell Host Microbe *8*, 422–432.

Hohenstein, A.C., and Roche, P.A. (2001). SNAP-29 is a promiscuous syntaxin-binding SNARE. Biochem. Biophys. Res. Commun. *285*, 167–171.

Hong, W. (2005). SNAREs and traffic. Biochim. Biophys. Acta *1744*, 120–144.

Itakura, E., Kishi-Itakura, C., and Mizushima, N. (2012). The hairpin-type tail-anchored SNARE syntaxin 17 targets to autophagosomes for fusion with endosomes/lysosomes. Cell *151*, 1256–1269.

Jackson, W.T., Giddings, T.H., Jr., Taylor, M.P., Mulinyawe, S., Rabinovitch, M., Kopito, R.R., and Kirkegaard, K. (2005). Subversion of cellular autophagosomal machinery by RNA viruses. PLoS Biol. *3*, e156.

Joubert, P.E., Meiffren, G., Grégoire, I.P., Pontini, G., Richetta, C., Flacher, M., Azocar, O., Vidalain, P.O., Vidal, M., Lotteau, V., et al. (2009). Autophagy induction by the pathogen receptor CD46. Cell Host Microbe *6*, 354–366.

Jounai, N., Takeshita, F., Kobiyama, K., Sawano, A., Miyawaki, A., Xin, K.Q., Ishii, K.J., Kawai, T., Akira, S., Suzuki, K., and Okuda, K. (2007). The Atg5 Atg12 conjugate associates with innate antiviral immune responses. Proc. Natl. Acad. Sci. USA *104*, 14050–14055.

Ke, P.Y., and Chen, S.S. (2011). Activation of the unfolded protein response and autophagy after hepatitis C virus infection suppresses innate antiviral immunity in vitro. J. Clin. Invest. *121*, 37–56.

Klionsky, D.J., Abdalla, F.C., Abeliovich, H., Abraham, R.T., Acevedo-Arozena, A., Adeli, K., Agholme, L., Agnello, M., Agostinis, P., Aguirre-Ghiso, J.A., et al. (2012). Guidelines for the use and interpretation of assays for monitoring autophagy. Autophagy 8, 445–544.

Kudchodkar, S.B., and Levine, B. (2009). Viruses and autophagy. Rev. Med. Virol. 19, 359–378.

Kyei, G.B., Dinkins, C., Davis, A.S., Roberts, E., Singh, S.B., Dong, C., Wu, L., Kominami, E., Ueno, T., Yamamoto, A., et al. (2009). Autophagy pathway intersects with HIV-1 biosynthesis and regulates viral yields in macrophages. J. Cell Biol. 186, 255–268.

Lee, J.H., Yu, W.H., Kumar, A., Lee, S., Mohan, P.S., Peterhoff, C.M., Wolfe, D.M., Martinez-Vicente, M., Massey, A.C., Sovak, G., et al. (2010). Lysosomal proteolysis and autophagy require presenilin 1 and are disrupted by Alzheimer-related PS1 mutations. Cell 141, 1146–1158.

Levine, B. (2005). Eating oneself and uninvited guests: autophagy-related pathways in cellular defense. Cell 120, 159–162.

Liang, C., Lee, J.S., Inn, K.S., Gack, M.U., Li, Q., Roberts, E.A., Vergne, I., Deretic, V., Feng, P., Akazawa, C., and Jung, J.U. (2008). Beclin1-binding UVRAG targets the class C Vps complex to coordinate autophagosome maturation and endocytic trafficking. Nat. Cell Biol. 10, 776–787.

Matsunaga, K., Saitoh, T., Tabata, K., Omori, H., Satoh, T., Kurotori, N., Maejima, I., Shirahama-Noda, K., Ichimura, T., Isobe, T., et al. (2009). Two Beclin 1-binding proteins, Atg14L and Rubicon, reciprocally regulate autophagy at different stages. Nat. Cell Biol. 11, 385–396.

Moreau, K., Ravikumar, B., Renna, M., Puri, C., and Rubinsztein, D.C. (2011). Autophagosome precursor maturation requires homotypic fusion. Cell 146, 303–317.

Nair, U., Jotwani, A., Geng, J., Gammoh, N., Richerson, D., Yen, W.L., Griffith, J., Nag, S., Wang, K., Moss, T., et al. (2011). SNARE proteins are required for macroautophagy. Cell 146, 290–302.

Nydegger, S., Foti, M., Derdowski, A., Spearman, P., and Thali, M. (2003). HIV-1 egress is gated through late endosomal membranes. Traffic 4, 902–910.

Ono, A., and Freed, E.O. (2004). Cell-type-dependent targeting of human immunodeficiency virus type 1 assembly to the plasma membrane and the multivesicular body. J. Virol. 78, 1552–1563.

Pelchen-Matthews, A., Kramer, B., and Marsh, M. (2003). Infectious HIV-1 assembles in late endosomes in primary macrophages. J. Cell Biol. 162, 443–455.

Shelly, S., Lukinova, N., Bambina, S., Berman, A., and Cherry, S. (2009). Autophagy is an essential component of Drosophila immunity against vesicular stomatitis virus. Immunity 30, 588–598.

Sir, D., Chen, W.L., Choi, J., Wakita, T., Yen, T.S., and Ou, J.H. (2008). Induction of incomplete autophagic response by hepatitis C virus via the unfolded protein response. Hepatology 48, 1054–1061.

Sir, D., Tian, Y., Chen, W.L., Ann, D.K., Yen, T.S., and Ou, J.H. (2010). The early autophagic pathway is activated by hepatitis B virus and required for viral DNA replication. Proc. Natl. Acad. Sci. USA 107, 4383–4388.

Steegmaier, M., Yang, B., Yoo, J.S., Huang, B., Shen, M., Yu, S., Luo, Y., and Scheller, R.H. (1998). Three novel proteins of the syntaxin/SNAP-25 family. J. Biol. Chem. 273, 34171–34179.

Su, Q., Mochida, S., Tian, J.H., Mehta, R., and Sheng, Z.H. (2001). SNAP-29: a general SNARE protein that inhibits SNARE disassembly and is implicated in synaptic transmission. Proc. Natl. Acad. Sci. USA 98, 14038–14043.

Takimoto, T., and Portner, A. (2004). Molecular mechanism of paramyxovirus budding. Virus Res. 106, 133–145.

Tanida, I. (2011). Autophagosome formation and molecular mechanism of autophagy. Antioxid. Redox Signal. 14, 2201–2214.

Tanida, I., Fukasawa, M., Ueno, T., Kominami, E., Wakita, T., and Hanada, K. (2009). Knockdown of autophagy-related gene decreases the production of infectious hepatitis C virus particles. Autophagy 5, 937–945.

Taylor, M.P., Burgon, T.B., Kirkegaard, K., and Jackson, W.T. (2009). Role of microtubules in extracellular release of poliovirus. J. Virol. 83, 6599–6609.

Tresse, E., Salomons, F.A., Vesa, J., Bott, L.C., Kimonis, V., Yao, T.P., Dantuma, N.P., and Taylor, J.P. (2010). VCP/p97 is essential for maturation of ubiquitin-containing autophagosomes and this function is impaired by mutations that cause IBMPFD. Autophagy 6, 217–227.

Wileman, T. (2007). Aggresomes and pericentriolar sites of virus assembly: cellular defense or viral design? Annu. Rev. Microbiol. 61, 149–167.

Wong, J., Zhang, J., Si, X., Gao, G., Mao, I., McManus, B.M., and Luo, H. (2008). Autophagosome supports coxsackievirus B3 replication in host cells. J. Virol. 82, 9143–9153.